

UNCLASSIFIED

SECURITY CLASSIFICATION OF THIS PAGE (When Data Entered)

REPORT DOCUMENTATION PAGE		READ INSTRUCTIONS BEFORE COMPLETING FORM												
1. REPORT NUMBER	2. GOVT ACCESSION NO.	3. RECIPIENT'S CATALOG NUMBER												
4. TITLE (and Subtitle)  ELECTRON IMPACT CROSS SECTIONS FOR MOLECULAR LASERS		5. TYPE OF REPORT & PERIOD COVERED Final - Technical 1 July 75 - 30 June 83												
		6. PERFORMING ORG. REPORT NUMBER												
7. AUTHOR(s)  Shek-Fu Wong, Principal Investigator		8. CONTRACT OR GRANT NUMBER(s)  N00014-76-C-0078												
9. PERFORMING ORGANIZATION NAME AND ADDRESS Yale University Applied Physics, P.O. Box 2159 Yale Station New Haven, CT 06520		10. PROGRAM ELEMENT, PROJECT, TASK AREA & WORK UNIT NUMBERS  NR 394-003												
11. CONTROLLING OFFICE NAME AND ADDRESS Office of Naval Research Physics Program Office (Code 421) Arlington, VA 22217		12. REPORT DATE 27 April 1984												
		13. NUMBER OF PAGES 30												
14. MONITORING AGENCY NAME & ADDRESS (if different from Controlling Office)		15. SECURITY CLASS. (of this report)  UNCLASSIFIED												
		15a. DECLASSIFICATION/DOWNGRADING SCHEDULE												
16. DISTRIBUTION STATEMENT (of this Report)  Approved for public release; distribution unlimited.														
17. DISTRIBUTION STATEMENT (of the abstract entered in Block 20, if different from Report)														
18. SUPPLEMENTARY NOTES														
19. KEY WORDS (Continue on reverse side if necessary and identify by block number)  <table border="0"> <tr> <td>electron impact experiments</td> <td>rotational excitation</td> <td>N<sub>2</sub></td> </tr> <tr> <td>cross sections</td> <td>vibrational excitation</td> <td>F<sub>2</sub>, Cl<sub>2</sub>, Br<sub>2</sub>, I<sub>2</sub></td> </tr> <tr> <td>threshold region</td> <td>dissociative attachment</td> <td>N<sub>2</sub><sup>*</sup>, HCl<sup>*</sup>, HF<sup>*</sup></td> </tr> <tr> <td>enhancement phenomena</td> <td>electronic excitation</td> <td>Ar, Kr</td> </tr> </table>			electron impact experiments	rotational excitation	N <sub>2</sub>	cross sections	vibrational excitation	F <sub>2</sub> , Cl <sub>2</sub> , Br <sub>2</sub> , I <sub>2</sub>	threshold region	dissociative attachment	N <sub>2</sub> <sup>*</sup> , HCl <sup>*</sup> , HF <sup>*</sup>	enhancement phenomena	electronic excitation	Ar, Kr
electron impact experiments	rotational excitation	N <sub>2</sub>												
cross sections	vibrational excitation	F <sub>2</sub> , Cl <sub>2</sub> , Br <sub>2</sub> , I <sub>2</sub>												
threshold region	dissociative attachment	N <sub>2</sub> <sup>*</sup> , HCl <sup>*</sup> , HF <sup>*</sup>												
enhancement phenomena	electronic excitation	Ar, Kr												
20. ABSTRACT (Continue on reverse side if necessary and identify by block number)  <p>This project deals with electron impact experiments on atoms and molecules relevant to the development of the N<sub>2</sub>-CO<sub>2</sub> and rare-gas halide lasers. Cross sections for state-to-state transitions in a variety of collisional processes (rotational, vibrational, and electronic excitation; dissociative attachment) have been determined in the first 4 eV of threshold and are generally found to exhibit great enhancement attributable to resonances. Highlights of the methods of cross-section measurement are also presented.</p>														

DD FORM 1 JAN 73 1473

EDITION OF 1 NOV 65 IS OBSOLETE

S/N 0102- LF-014-6601

UNCLASSIFIED

SECURITY CLASSIFICATION OF THIS PAGE (When Data Entered)



Final Technical Report

ELECTRON IMPACT CROSS SECTIONS FOR MOLECULAR LASERS

by

Shek-Fu Wong  
Principal Investigator

Prepared for  
Office of Naval Research  
Physics Program Office  
Arlington, Virginia 22217

Contract No. N00014-76-C-0078  
From 1 July 1975 to 30 June 1983

Approved for public release; distribution unlimited

YALE UNIVERSITY

## TABLE OF CONTENTS

	Page
I. INTRODUCTION	1
II. CROSS SECTIONS FOR THE $N_2$ - $CO_2$ LASER	3
III. CROSS SECTIONS FOR THE RARE-GAS HALIDE LASERS	12
IV. PUBLICATIONS UNDER ONR SPONSORSHIP	28
V. REFERENCES	29

## I. INTRODUCTION

A laser is an oscillator that converts input energy, through an amplifying medium, into coherent radiation of extremely well defined direction and spectrum. Together, these characteristics and their potential for enormous power output render lasers vital to modern technologies such as long-range communication and surveillance, isotope separation, and controlled thermonuclear fusion.

Among all kinds of lasers, the gaseous discharge lasers have been found to be very promising in efficient high-power operation over a wide range of wavelengths. In such lasers the amplifying medium is a gas plasma excited by electric discharges into population inversion between 2 energy levels. Through stimulated emission the molecules in the upper level decay to the lower level, converting their excess energy into laser radiation. Clearly, an understanding of the kinetics of the electric discharges plays a key role in laser advancement; and the need of such understanding demands a comprehensive study of electron collisions in terms of the pertinent cross sections.

To date, the gaseous discharge lasers widely studied include the  $N_2-CO_2$  laser operated at infrared wavelengths and the rare-gas halide lasers which give off ultraviolet radiation. The advent of these lasers in the past two decades has since stimulated a world-wide interest and substantial cross sectional data have been accumulated (Kieffer, 1973; McDaniel et al, 1977). Many such data important to the laser design, however, remain unavailable as these measurements pose stringent experimental requirements such as the incorporation of a source of excited molecules into an electron impact spectrometer, high energy-resolution, and controlled detection of slow electrons.

During the current period from 1975 to 1983, we have directed our effort to develop the necessary experimental techniques and devices and to carry out further measurements on electron impact cross sections relevant to these infrared and ultraviolet lasers. Our experimental results are highlighted in the body of this report as their details can mostly be referred to the published articles listed in the text.

## II. CROSS SECTIONS FOR THE $N_2$ - $CO_2$ LASER

In this infrared laser the efficient conversion of electrical to optical energy relies on the effective transfer of the kinetic energy of the plasma electrons to the vibrational excitation of  $N_2$ . The excess energies of these molecules are subsequently funnelled, via  $N_2$ - $CO_2$  collisions, into the upper energy level of the laser for stimulated radiation.

The cross sections for vibrational excitation by electron impact on  $N_2$  in the ground vibrational state have been extensively measured. They show great magnitudes ( $10^{-16} \text{ cm}^2$ ) and oscillatory energy structures around 1-4 eV due to the formation of a shape resonance of  $^2\Pi_g$  symmetry (reviewed by Schulz, 1976).

Like vibrational excitation from the ground state, such process from nuclear-excited states as well as pure rotational excitation of  $N_2$  can affect the energy flow in the gaseous discharge and eventually the laser performance. Whereas theoretical calculations on these cross sections have been substantial (Chandra and Temkin and references therein, 1976), experimental studies in these 2 areas have so far been confined to pure rotational excitation with the electron swarm method for collisional energies below 1 eV (reviewed by Phelps, 1968). Consequently, in the present period we have carried out electron beam experiments on these vibrational and rotational excitation processes with energy range specifically in the 1-4 eV resonant region.

### A. Vibrational Excitation of Nuclear-Excited $N_2$

For vibrational excitation by electron impact on nuclear-excited  $N_2$ , we have studied the absolute differential ( $90^\circ$ ) and integral cross sections of the  $v=1-2$  transition in the energy range 1-4 eV (Wong, Michejda, and Stamatović, 1977).

The measurement of these cross sections poses an experimental challenge due to the difficulties in combining the generation of an intense beam ( $10^{13} \text{ cm}^{-3}$ ) of nuclear-excited molecules with high-resolution ( $10^{-2}$  eV) electron impact spectrometers. We have overcome this technical barrier through the development of a constricted-discharge tube to facilitate the excited-molecule production, and through the use of a metal-channel exit to prevent the escape of the plasma electrons which can cause serious background problems.

The apparatus employed in the present study is given in Fig. 1. This is the same electron impact spectrometer as in our earlier experiments on

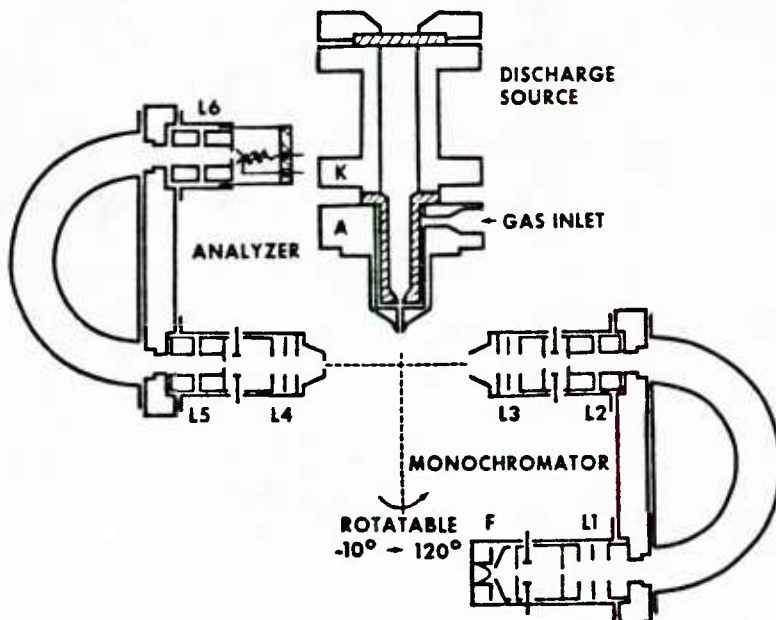


Fig. 1. Hemispherical electron impact spectrometer with discharge molecular-beam source.  
(From Wong et al, 1977.)



vibrational excitation of ground-state molecules (Wong and Schulz, 1974), but with the gas nozzle replaced by the newly developed discharge tube. The basic components of the spectrometer include a rotatable hemispherical monochromator to form a beam of monoenergetic electrons and a fixed hemispherical analyzer to examine the angle and kinetic energy of the scattered electrons. Regarding the discharge tube, it consists of an aluminum cathode K, a molybdenum anode A, and a ceramic spacer to constrict the gaseous discharge on top of a source channel in the anode. Through this channel the gas plasma exits to form a beam of molecules, crossing the path of the primary electron beam. The populations of the molecules in different vibrational states ( $v=0, 1, 2, \dots$ ) are measured on site using a threshold electronic excitation technique (Michejda, 1977). At a source pressure of 2 Torr and a discharge current of 20 mA, the molecular beam density is  $2 \times 10^{14} \text{ cm}^{-3}$ , with typically 12% population in the excited  $v=1$  state, and the rest mostly in the ground  $v=0$  state. For all measurements a spectrometer resolution (FWHM for energy-loss peaks) of 35 meV and a scattering angle of  $90^\circ$  are used. The maximum count rate for the  $v=1-2$  transition is  $1 \times 10^3$  cps, with less than 0.5% background contribution.

To determine the absolute  $v=1-2$  differential cross sections over 1-4 eV, we first measure the relative  $v=1-2$  differential cross sections in the same energy range and then normalize them to yield the absolute scale.

The relative  $v=1-2$  differential cross sections are obtained via measurement of the energy dependence of the count rate of the scattering electrons which have energy-loss corresponding to the  $\Delta v=1$  excitation, with the discharge on and off. The present spectrometer resolution permits the separation of the  $\Delta v=1$  from the other  $\Delta v$  contributions, as exemplified in the energy-loss spectrum



at 1.87 eV given in Fig. 2. Hence, when the discharge is on, the measured energy dependence contains contributions predominantly from both  $v=0-1$  and  $v=1-2$ ; but when the discharge is off it is contributed only by  $v=0-1$ . As a result the difference of the on and off energy dependences, weighed with appropriate factors of vibrational populations, gives the energy dependence for the  $v=1-2$  transition. Further, since both the  $v=0-1$  and  $v=1-2$  energy dependences are obtained under the condition of

constant electron-beam intensity and analyzer transmission, they also represent the relative  $v=0-1$  and  $v=1-2$  differential cross sections in the energy range of observation.

The absolute scale of the  $v=1-2$  differential cross sections is determined at 2.27 eV by first normalizing at this energy the  $v=0-1$  differential cross section to the absolute He elastic differential cross section which is calculated by LaBahn and Callaway (1970). In this step the scattering intensity of the  $v=0-1$  excitation in  $N_2$  and that of elastic scattering in He are measured at the same selected impact energy and source pressure (under the molecular-flow condition). By multiplying the ratio of these 2 scattering intensities to the known elastic differential cross section in He, we obtain the absolute vibrational differential cross section. The resulted absolute scale for  $v=0-1$  also applies to that for  $v=1-2$  because they both have the same relative scale.

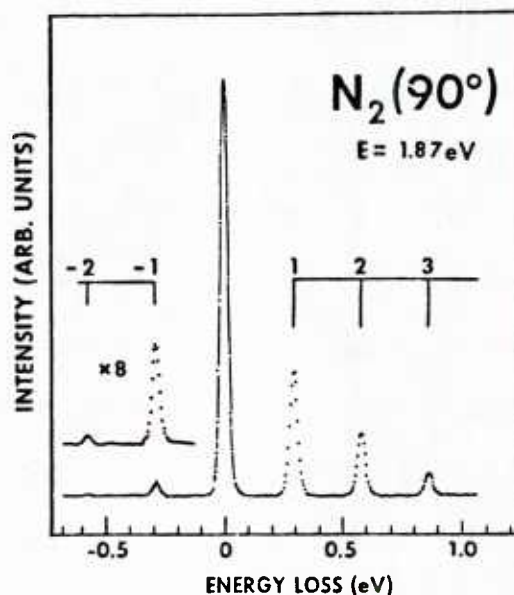


Fig. 2. Energy-loss spectrum in  $N_2$  with discharge on.  
(From Wong et al, 1977.)

Our findings on the absolute  $v=1-2$  differential cross sections in the energy range 1-4 eV are shown in Fig. 3. These cross sections are characterized

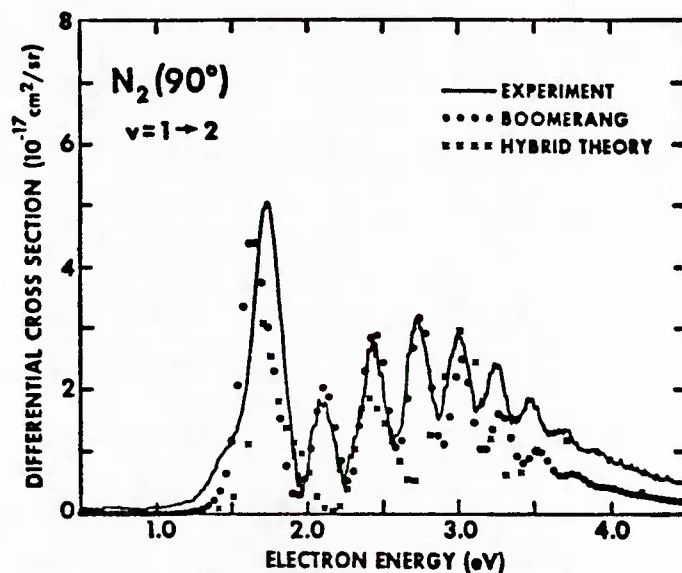


Fig. 3. Absolute vibrational differential cross section of  $N_2$  in 1-4 eV. (From Wong et al, 1977.)

by a strong sharp peak at 1.7 eV, followed by a series of weaker peaks having a bell-shaped profile centered near 2.7 eV. Compared to those for  $v=0-1$ , the cross sections for  $v=1-2$  show a similar overall magnitude and energy spacings of the peaks, but a different gross shape. All these phenomena indicate that the  $^2\Pi_g$  shape resonance in  $N_2$ , responsible for the vibrational excitation of the ground state ( $v=0-1$ ) is also dominant in the vibrational excitation of the excited state ( $v=1-2$ ).

For determination of the  $v=1-2$  integral cross sections over 1-4 eV, we have followed a special procedure since the excitation is dominated by a single shape resonance. Under this circumstance the angular distribution of the inelastically scattered electrons is independent of incident energy throughout

the resonant region and has been well studied and documented (Read and references therein, 1972). By dividing the known angular distribution due to the  $^2\Pi_g$  shape resonance at  $90^\circ$  into the integrated value of this distribution over all angles, we obtain the constant conversion factor, which is  $4\pi \times 14/15$ . The products of this factor and our measured  $v=1-2$  differential cross sections at  $90^\circ$  give the corresponding integral cross sections, in which the maximum magnitude is  $(5.9 \pm 1.5) \times 10^{-16} \text{ cm}^2$  at 1.7 eV.

The absolute  $v=1-2$  differential cross sections of  $N_2$  have been calculated by Dubé and Herzenberg with the boomerang model (1975) and by Chandra and Temkin with the hybrid theory (1976). Their findings are also given in Fig. 3 together with our measurements for comparison. There is an excellent agreement between the present experiment and the boomerang calculation in the maximum magnitude of the cross sections. Regarding the shape of the cross sections, both the measured and calculated results are in accord within the first 3 eV but the latter falls off notably faster at higher energies. On the other hand, our results agree only grossly in the shape of the cross sections with the hybrid calculation and the measured overall magnitude is about a factor of 2 greater.

## B. Rotational Excitation of N<sub>2</sub>

In this study we have determined the absolute differential (60°) and integral cross sections for excitation of the rotational branches  $\Delta j = \pm 4$  in N<sub>2</sub> at 300 °K, over electron incident energies 1-4 eV (Wong and Dubé, 1978).

The electron impact spectrometer which we adopt for these rotational excitation experiments has been described in the previous section. A conventional single-channel gas nozzle, however, is used to generate the molecular beam at 300 °K. The spectrometer resolution, 18 meV, is close to the energy spacings of the rotational branches ( $\Delta j = 0, \pm 2$ , and  $\pm 4$ ) of N<sub>2</sub> and permits direct observation of the  $\Delta j = \pm 4$  contributions for initial  $j$  values greater than 12. Under this resolution the electron beam current is about 1 nA and the maximum signal for elastic scattering is  $1 \times 10^3$  cps.

To study the rotational excitation in the energy range of 1-4 eV, we first measured electron energy-loss spectra at a fixed impact energy over scattering angles 30-90° to reveal the contributions from different rotational branches. Examples of such spectra are presented in Fig. 4. By recording the variation with impact energy over 1-4 eV of the signal intensities corresponding to energy losses greater than  $\pm 30$  meV, under constant electron-beam current and analyzer transmission, we then obtain the relative

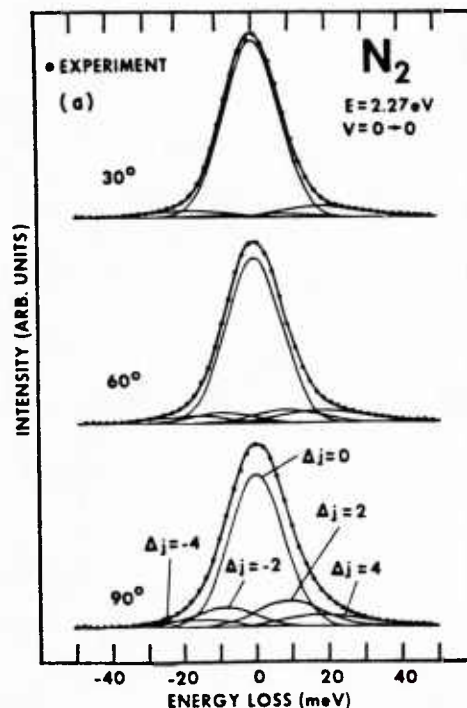


Fig. 4. Energy-loss spectrum in N<sub>2</sub> at 2.27 eV.  
(From Wong and Dubé, 1978.)

differential cross sections for excitation to the  $\Delta j = \pm 4$  branches in the energy range studied.

The relative differential cross sections thus obtained are normalized to the absolute scales at an electron energy of 2.27 eV and a scattering angle of  $60^\circ$  as in the following. First, the energy-loss spectrum measured at this energy and angle is profile fitted to extract the relative contributions of all rotational branches (see Fig. 4) and from which the fractional contributions of the  $\Delta j = \pm 4$  branches are derived. Second, by measuring the rotationally unresolved elastic signal in  $N_2$  and by using the He normalization procedure as described earlier in Section A, we obtain the total differential cross section for all the rotational branches. The products of the results of the first and second steps gives the absolute  $\Delta j = \pm 4$  differential cross sections at 2.27 eV, which in turn determine the 2 absolute scales of the relative  $\Delta j = \pm 4$  differential cross sections.

We find that over 1-4 eV the absolute differential cross sections for  $\Delta j = \pm 4$  are related to each other in accord with the principle of detailed balancing, and thus only the experimental results on  $\Delta j = 4$  is given in Fig. 5.

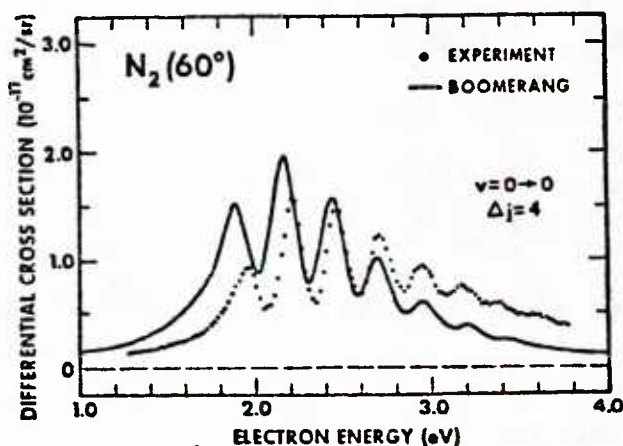


Fig. 5. Absolute  $\Delta j = 4$  differential cross sections of  $N_2$  in 1-4 eV.  
(From Wong and Dube, 1978.)

From this figure it is evident that for  $\Delta j=4$  the cross sections exhibit a large magnitude ( $10^{-17} \text{ cm}^2/\text{sr}$ ) and many overlapping, equally spaced peaks in the form of a bell-shaped envelope. The position of the maximum peak is at 2.2 eV. These phenomena are analogous to those previously observed in vibrational excitation of the ground state over 1-4 eV which is dominated by the  $^2\Pi_g$  shape resonance, and thus indicating that the rotational excitation is likewise dominated by this shape resonance within the same energy range. As an additional check for this implication, we have measured the angular dependences for the  $\Delta j=\pm 4$  branches at 2.27 eV over  $30-90^\circ$  at 10 degree intervals and find that they are to within experimental errors of 25% in agreement with those predicted for their excitation via the  $^2\Pi_g$  shape resonance (Read, 1972).

For determination of the integral cross section for  $\Delta j=\pm 4$ , the special procedure previously applied for vibrational excitation (see Section A) is adopted. Through this procedure, the conversion factor at  $60^\circ$  is derived to be  $4\pi \times 1.6$  for both branches while the maximum integral cross section is  $(2.1 \pm 0.8) \times 10^{-16} \text{ cm}^2$  for  $\Delta j=4$  at 2.2 eV.

Using their boomerang model, Dube and Herzberg (1975) have calculated the absolute  $\Delta j=4$  differential cross sections and the results are given in Fig. 5 for comparison with our experimental findings. Both the measurements and the calculations agree very well in the fine energy-structures and in the overall absolute magnitude of the cross sections. However, the calculated cross sections are greater at energies below 1.9 eV but smaller at energies above 3 eV.



### III. CROSS SECTIONS FOR THE RARE-GAS HALIDE LASERS

The rare-gas halide lasers were discovered in the mid 1970s, about a decade later than the infrared  $\text{N}_2\text{-CO}_2$  laser. Operated on electronic transitions these laser systems emit ultraviolet radiation via stimulated emission of excited rare-gas halide molecules. Such molecules are formed principally via one of the two channels, namely the ion channel in which halogen negative ions recombine with rare-gas positive ions and the neutral channel in which rare-gas excited atoms react with halogen species (for a review see Brau, 1979).

In the ion channel, the negative ions are generated from dissociative electron attachment to molecules containing halogen atoms; whereas in the neutral channel, the excited atoms are produced primarily through electronic excitation in electron collisions with rare-gas atoms. Hence, these 2 processes, dissociative attachment and electronic excitation, both directly affect the energy flow in the course of the excited-molecule formation and subsequently the efficiency as well as the stability of the laser systems.

The significance of these 2 collision processes in laser operation and a dearth of data on their cross sections have motivated our research efforts along this direction. In the present period we have carried out electron impact experiments on: A. Dissociative attachment to halogen-containing molecules and B. Electronic excitation of Kr and Ar. In these experiments the impact energies we have focussed on are the first several electron volts of the lowest attachment and excitation thresholds; as at such energies the electron population in the laser plasmas are often relatively large and the collisional cross sections there are expected to be strongly enhanced due to the presence of resonances.



### A. Dissociative Attachment to Halogen-Containing Molecules

Among the halogen-containing molecules that occur commonly in the plasmas of the rare-gas halide lasers, we have chosen  $F_2$ ,  $Cl_2$ ,  $Br_2$ , and  $I_2$  as well as nuclear-excited HCl and HF for the present experiments on dissociative attachment.

#### 1) $F_2$ , $Cl_2$ , $Br_2$ , and $I_2$

In this study we have measured the energy dependence of the cross sections for  $F^-/F_2$ ,  $Cl^-/Cl_2$ ,  $Br^-/Br_2$ , and  $I^-/I_2$  at gas temperature of 400 °K in the energy range of 0-8 eV (Tam and Wong, 1978).

Halogens are well known to be extremely reactive. This feature renders electron impact experiments on dissociative attachment of these molecules vulnerable to impurity contribution and cutoff of electron beam at low impact energies. As a result, uncertainties existed in the previous experimental cross sections (reviewed by Massey, 1976).

To deal with these problems we have employed an electron impact mass spectrometer designed by Stamatović and Schulz (1970) with modification. The gas cell of this spectrometer is replaced with a cylindrical iridium oven as the collision chamber. The great inertness of this collision chamber to chemical reaction has enabled us to study all the 4 halogens with the incident electron-beam controlled to essentially zero impact energy. The impurities in the target gas are monitored, in situ, by observing the mass spectrum of the positive ions generated by electron impact ionization and are found to be mainly hydrogen halides. After a passivation period from several hours for  $I_2$ ,  $Br_2$ , and  $Cl_2$  and to 2 days for  $F_2$ , the gas becomes pure and remains uncontaminated during the course of the experiments.

A schematic view of the modified apparatus is shown in Fig. 6. During an experiment monoenergetic electrons produced by a trochoidal monochromator are collimated by an uniform magnetic field to bombard the target gas in the iridium oven. Negative ions produced from dissociative electron attachment are mass

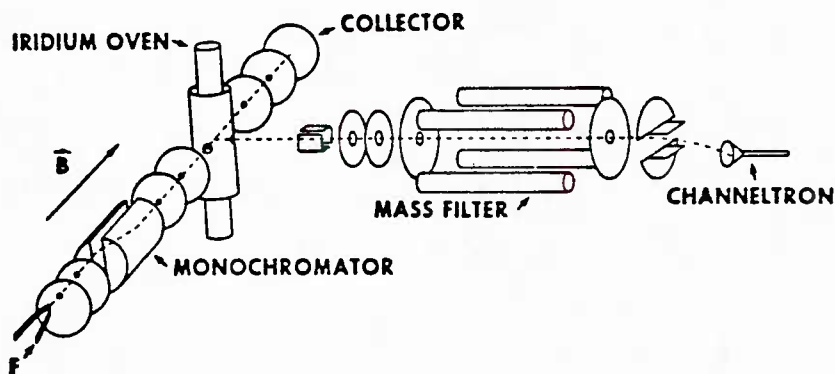


Fig. 6. Electron-impact mass spectrometer with iridium oven.  
(From Wong, 1979.)

analyzed at right angles with a quadrupole filter and then detected with a channeltron. A constant electron beam current of  $1 \times 10^{-8}$  A is maintained from 10 eV down to typically  $0.05 \pm 0.05$  eV.

The energy dependence of the cross sections for dissociative attachment in a selected halogen is measured from the variation with electron impact energy of the count rate for the mass-identified negative ion, under the conditions of constant electron beam intensity and ion transmission. Further, all the peak structures observed in the energy dependence spectrum are checked for their required linear dependence on gas pressure, thereby insuring that the measured cross sections are entirely due to the process of dissociative attachment.

Our measured cross sections for  $F^-/F_2$ ,  $Cl^-/Cl_2$ ,  $Br^-/Br_2$ , and  $I^-/I_2$  over 0-8 eV are shown in Fig. 7. The common feature among the 4 halogen molecules is a sharp peak at zero energy. At higher energies 2 broad peaks appear in  $Cl_2$ ,  $Br_2$ , and  $I_2$ . As the mass of the halogen molecule increases, the 2 broad peaks shift down in energy and lie closer with each other; while their intensities relative to the zero-energy peak grows stronger.

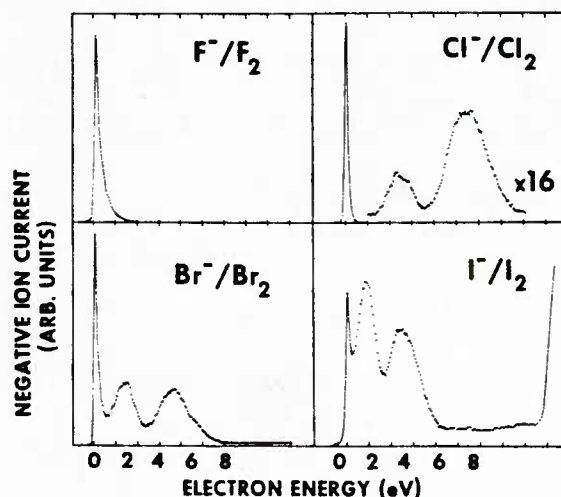


Fig. 7. Energy dependences of dissociative attachment to halogens.  
(From Tam and Wong, 1978.)

The energy locations of all these dissociative attachment peaks are listed in Table 1. Also included are other reported data of the similar experiments. In comparison with the earlier work, the present results reveal most of the

TABLE I. Comparison of dissociative attachment peaks in halogen molecules.

Ion	Peak energy (eV) <sup>a</sup>			
	Present	Previous work		
$F^-/F_2$	$0.09 \pm \begin{smallmatrix} 0.05 \\ 0.09 \end{smallmatrix}$	$< 2.0^b$	$1.2^c$ $6.0$	$1.2^d$ $7.0$ $9.5$
$Cl^-/Cl_2$	$0.03 \pm \begin{smallmatrix} 0.05 \\ 0.03 \end{smallmatrix}$ $2.5 \pm 0.15$ $5.5 \pm 0.15$	$< 2.0^b$ $4.4 \pm 0.2$	$2.4 \pm 0.1^e$	Zero energy <sup>f</sup> $2.5 \pm 0.05$ $5.76 \pm 0.05$
$Br^-/Br_2$	$0.07 \pm \begin{smallmatrix} 0.05 \\ 0.07 \end{smallmatrix}$ $1.4 \pm 0.15$ $3.7 \pm 0.15$	$2.8^e$	$0.03 \pm 0.03^g$	
$I^-/I_2$	$0.05 \pm 0.05$ $0.9 \pm 0.10$ $2.5 \pm 0.10$	$0.4^h$	$0.34 \pm 0.07^g$	Zero energy <sup>i</sup>

(From Tam and Wong, 1978.)

peaks reported, though there are some discrepancies in their exact locations. Further, we uncover a new peak in each of the halogen molecules, namely a zero energy spike in  $F_2$  and  $Cl_2$  and a higher energy peak in  $Br_2$  and  $I_2$ . On the other hand, a concurrent experiment has been performed by Kurepa and Belic<sup>1</sup> (1977) on  $Cl_2$  and their findings (referenced as f in Table 1) are in good agreement with our results.

## 2) Nuclear-Excited HCl and HF

Experiments on dissociative attachment by electron impact on HCl (Ziesel et al, 1975) and HF (Abouaf and Teillet-Billy, 1980) were restricted to their ground vibrational states, leaving the excited states unexplored. To pursue this new area, we have determined for  $\text{Cl}^-/\text{HCl}$  and  $\text{F}^-/\text{HF}$  respectively the dependence of the threshold attachment cross section on the initial vibrational states:  $v=0, 1$ , and  $2$ . A similar experiment has also been performed on  $\text{Cl}^-/\text{DCl}$  to examine the isotope effect on the  $\text{Cl}^-/\text{HCl}$  cross sections (Allan and Wong, 1981).

The apparatus used for this study is the same as that for the halogen experiments, but with the ion optics redesigned for better detection efficiency. The iridium oven is operated at high temperatures, up to  $1180^\circ\text{K}$ , to thermally populate the target molecules in different nuclear-excited states. The electron-beam resolution is  $50\text{ meV}$  which permits separation of ion signals from the individual vibrational-excited states.

The vibrational-state dependence of the attachment cross section for a selected hydrogen halide is derived from the measured spectra of negative-ion formation by  $0\text{--}4\text{ eV}$  electrons in that gas, at several temperatures between  $300$  and  $1180^\circ\text{K}$ . We shall use our results on  $\text{Cl}^-/\text{HCl}$  as shown in Fig. 8 to illustrate the derivation procedures. The  $300^\circ\text{K}$  spectrum, which consists of a steep peak at  $0.82\text{ eV}$ , represents the threshold electron

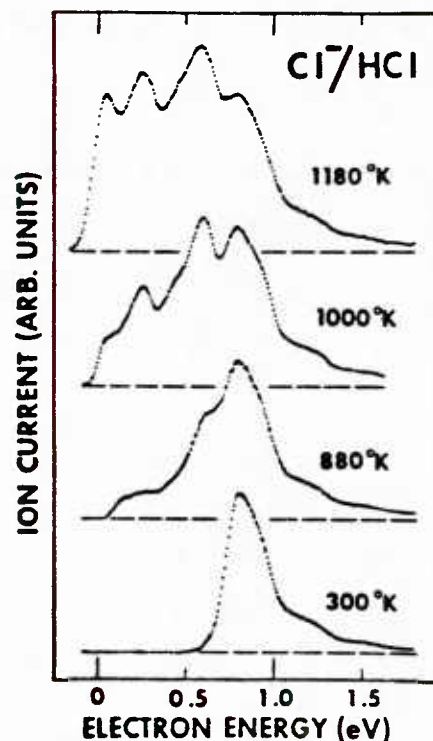


Fig. 8. Energy dependences for  $\text{Cl}^-/\text{HCl}$ .  
(From Allan and Wong, 1981.)

attachment to the lowest dissociation limit of  $\text{Cl}^- + \text{H}$  from the ground  $v=0$  state of  $\text{HCl}$ . The spectra obtained at higher temperatures contain additional peaks at lower energies, and the magnitude of these peaks becomes larger as the temperature is raised. These temperature-dependent peaks are due to  $\text{HCl}$  in the excited rotational manifold of different vibrational states ( $v=0, 1$ , and  $2$ ), which takes less electron energy to reach the same dissociation limit. By dividing the peak contributions from each vibrational states with their corresponding thermal populations, we obtain the relative threshold attachment cross sections for the individual states.

Our findings on these threshold cross sections for the 3 lowest vibrational states of  $\text{HCl}$ ,  $\text{DCl}$ , and  $\text{HF}$  are summarized in Table 2. Common to all these molecules is the feature of an order-of-magnitude enhancement in cross section with each increase of vibrational quantum. The largest vibrational enhancement, however, is observed in  $\text{Cl}^-/\text{HCl}$ . Using the known

absolute magnitude for the  $v=0$  state as a standard (reference b in Table 2), we find that the  $\text{Cl}^-$  cross section for the  $v=2$  state is  $(7.8 \pm 4.7) \times 10^{-15} \text{ cm}^2$  at threshold. This magnitude is a fraction of the wavelength-limited cross section for the incident electron, indicating the great efficiency of dissociative attachment to vibrationally excited  $\text{HCl}$ .

TABLE 2 Vibrational enhancement in threshold cross section of dissociative attachment.<sup>a, b</sup>

	HCl	DCl	HF
$\sigma_{v=1}/\sigma_{v=0}$	38	32	21
$\sigma_{v=2}/\sigma_{v=0}$	880	580	300

<sup>a</sup>Experimental errors are  $\pm 30\%$  for  $v=1$  and  $\pm 50\%$  for  $v=2$  for the ratios tabulated above.

<sup>b</sup>The peak cross sections for ground-state ( $v=0$ )  $\text{HCl}$  and  $\text{DCl}$  were determined to be  $8.9 \times 10^{-18} \text{ cm}^2$  and  $1.8 \times 10^{-18} \text{ cm}^2$ , respectively, by Azria *et al.* (Ref. 21).

(From Allan and Wong, 1981.)

## B. Electronic Excitation in Heavy Rare-Gas Atoms: Kr and Ar

Early experimental studies in electronic excitation of Kr and Ar dealt mainly with cross sections for total excitation, metastable production or photon emission (for a review see Bransden and McDowell, 1978). With recent advancement in the energy resolution and sensitivity of electron impact spectrometers, such studies have been extended to differential cross sections for excitation of individual electronic energy levels in both atoms.

For impact energy from 100 to about 4 eV above the lowest threshold, electronic differential cross sections over a wide range of scattering angles have been measured in Kr by Trajma et al (1981) and in Ar by Chutjian and Cartwright (1981). For energy within 0-4 eV of threshold, however, such cross sections have been studied only qualitatively in terms of excitation function measurements (Swanson et al, 1973). The lack of quantitative data on such low energy studies have thus stimulated our research endeavor in this area during the present contract period. In addition to acquiring the necessary experimental techniques, we have carried out initial experiments on near-threshold electronic excitation in these 2 atoms.

### 1) The Lowest 4 Excited Energy Levels in Kr

In Kr we have measured the relative differential cross sections for excitation to the individual  $4p^5s$  ( $^3P_2$ ,  $^3P_1$ ,  $^3P_0$ , and  $^1P_1$ ) levels within the first 4 eV of threshold, for scattering angles of  $30^\circ$ ,  $55^\circ$ , and  $90^\circ$ . An estimate of the absolute magnitudes of these differential cross sections has also been made (Phillips, Ph.D. thesis, 1981).



The apparatus for this study is a hemispherical electron impact spectrometer, which has been employed earlier in the vibrational excitation experiments as described in Chapter II. The present energy resolution, 45 meV, for both the monochromator and the analyzer, is sufficient to resolve the 4 energy levels investigated. The maximum electron scattering signal for these electronic excitation is about 300 cps.

Apart from the energy resolution and sensitivity requirements, another condition crucial to measurement of electronic differential cross sections in the threshold region is the uniformity of the analyzer transmission for the inelastically scattered electrons down to the lowest possible energy.

In experiments dealing with the transmission of slow electrons, it is essential to eliminate all stray electrostatic and magnetic fields in the collision region. Prior to the present experiments, through the incorporation of an molybdenum grid shield in this region inside the conventional mu-metal shield, we had greatly reduced these 2 fields there and were able to detect the scattered electrons down to zero energy (Wong et al, 1977). However, the uniformity of the analyzer transmission below 0.7 eV remained unestablished. Since the scattered electrons with such low energies are very sensitive to the residual electrostatic fields due to surface contamination of the collision region, special attention has been made on improving the surface conditions there. This includes replacing the oil diffusion pump with a turbomolecular pump to reduce oil vapor contamination, heating the collision region to 460 °K for less surface adsorption of background gases and finally modifying the molybdenum grid shield from a gauge to a spiral configuration to facilitate outgassing during the experiments.



To determine the analyzer transmission as a function of electron energy, we adopt as a standard the continuum generated by near-threshold electron impact ionization in He (Pichou et al, 1976). In such ionization process the continuum consists of isotropically scattered electrons in uniform energy distribution. Thus the deviation of the measured continuum spectrum from the expected uniform distribution gives the analyzer transmission function at the angle studied. An example of such measurement is shown in Fig. 9, and the transmission function obtained is uniform to within  $\pm 20\%$  over the energy range of 3.5 to 0.1 eV.

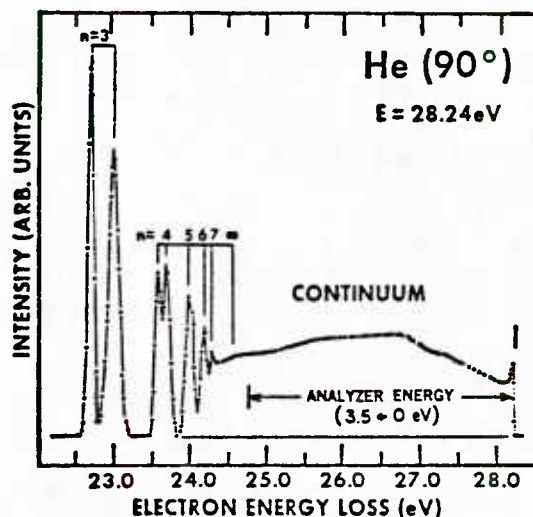


Fig. 9. Energy-loss spectrum for the He ionization continuum. (From Phillips and Wong, 1981.)

Because of the weak electron signals in the experiments on the near-threshold ionization, it is very time consuming to measure the continuum spectrum before and after each experiment. To expediate the process of calibrating the analyzer transmission function, we have taken advantage of the strong electron signals in the near-threshold excitation of the  $2^3S$  level in He. This involves the measurement of the energy dependence of the He  $2^3S$  cross sections under the same analyzer condition as in the measurement of the ionization continuum. The He cross sections thus obtained serve as a secondary standard to derive the transmission function in the Kr experiments (Phillips and Wong, 1981).

The relative electronic differential cross sections in Kr are determined as follows: First, the current of the primary electron beam and the count rate for electrons scattered into a selected angle with energy-loss equal the excitation energy of a selected level are measured simultaneously as the impact energy is scanned. Second, a small background due to stray electrons is subtracted from the count rate to yield the scattering signal intensity. Finally, by dividing this intensity with the electron beam current and the analyzer transmission, the energy dependence of the differential cross sections for that level is obtained. These procedures are applied to the  $3p_2$ ,  $3p_1$ ,  $3p_0$ , and  $1p_1$  levels in turn under the same gas pressure and analyzer tuning voltages to obtain their relative magnitudes within 0-4 eV of threshold.

For the 3 scattering angles studied, we find that the energy dependences of the  $3p_2$ ,  $3p_1$ ,  $3p_0$ , and  $1p_1$  levels are generally dominated by a broad peak at 1.2 eV above threshold in addition to many sharp structures. Figs. 10 and 11

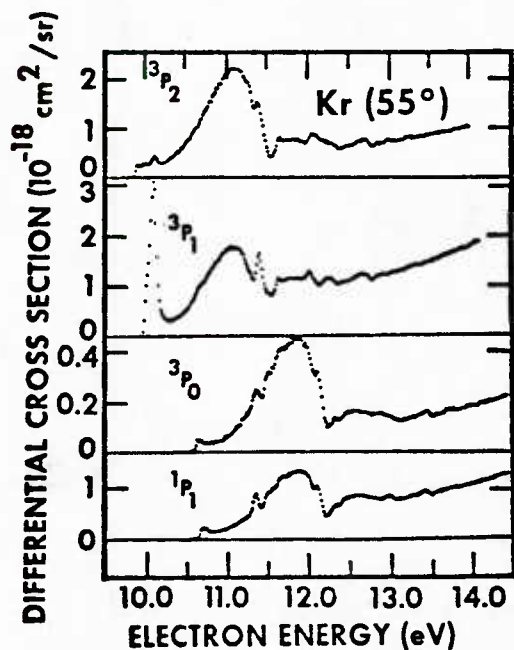


Fig. 10. Electronic differential cross sections in Kr at  $55^\circ$ .  
(From Phillips, Ph.D. thesis, 1981.)

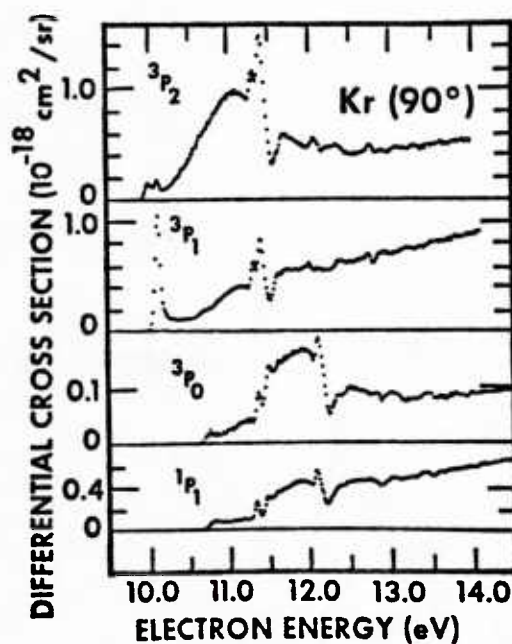


Fig. 11. Electronic differential cross sections in Kr at  $90^\circ$ .

give examples of these energy dependences at  $55^\circ$  and  $90^\circ$ . The energy positions of these peaks and structures are generally consistent with those reported by Swanson et al (1973). Nevertheless, with known analyzer transmission employed in the present investigation, we uncover 2 correlation phenomena among the cross sections of these 4 levels.

As evident in Figs. 10 and 11, the gross shapes of the differential cross sections for the 2 metastable levels ( $^3P_2$  and  $^3P_0$ ) mimic each other; so do those for the 2 UV emitting levels ( $^3P_1$  and  $^1P_1$ ). For any impact energy above threshold (except at threshold or near strong sharp structures) the ratio of the cross sections for the metastable levels is  $(5.6 \pm 1.1):1$  while that for the 2 UV emitting levels is  $(1.4 \pm 0.3):1$ . It is interesting to find that the cross section ratio for the 2 metastable levels are in accord with the ratio of their respective degeneracy factors, but not for the 2 UV emitting levels.

The absolute electronic differential cross section of Kr,  $(\frac{d\sigma}{d\Omega})_{Kr}$ , at a selected angle and energy above threshold can be obtained by using the following normalization formula:

$$(\frac{d\sigma}{d\Omega})_{Kr} = (\frac{d\sigma}{d\Omega})_{He} \cdot \frac{C_{Kr}}{C_{He}} \cdot \frac{I_{He}}{I_{Kr}} \cdot \frac{P_{He}}{P_{Kr}}$$

where  $(\frac{d\sigma}{d\Omega})_{He}$  is the absolute elastic differential cross section of He (O'Malley et al, 1979) at that angle and at an electron impact energy equal to that energy.  $C_{Kr}$  and  $C_{He}$  are the count rates measured for the electronic excitation and the elastic processes obtained under identical analyzer tuning conditions;  $I_{Kr}$  and  $I_{He}$  the intensities of the primary electron beams, and finally  $P_{Kr}$  and  $P_{He}$  the gas pressures in the target source. Using this formula, we have

normalized the  $^3P_1$  differential cross sections at 2.8 eV and 3.4 eV above threshold, for each of the 3 angles studied. Through these results the absolute scales for all the 4 electronic levels are determined and examples of these absolute scales for  $55^\circ$  and  $90^\circ$  are contained in Figs. 10 and 11.

In this normalization method, the formula is derived under the assumption that the ratio of the 2 source pressures of different gases equals that of the 2 densities of the corresponding target beams. This assumption has been shown to be valid only when the source is operated at low pressures, under the molecular-flow condition (reviewed by Trajmar and Register, 1980). In the present experiment, however, the demanding sensitivity requirement has resulted in the use of high pressures, namely 1 Torr of Kr and He for a source channel of  $0.65 \times 7.5$  mm. These render the operation on 2 equal source pressures of different gases and under the transition-flow condition in which the validity of the normalization formula is uncertain. Thus the absolute scales shown in Figs. 10 and 11 as well as in the thesis for Kr may contain a systematic error in the pressure factor and await further studies to ascertain their accuracies.

The pressure problem encountered in our normalization experiment on Kr can be avoided by using a procedure similar to that of Trajmar et al (1981). This involves the normalization of the Kr electronic cross sections to Kr elastic cross sections which are in turn normalized to the absolute He elastic cross sections. The electronic-to-elastic normalization deals with the same gas and can be carried out under identical pressure to satisfy the assumption of the formula even under transition flow. As to the elastic-to-elastic normalization between Kr and He, the much larger elastic signals make possible operation under molecular flow and presents no pressure problem in normalization.

## 2) The Lowest 3 Excited Energy Levels in Ar

In this initial study of electronic excitation in Ar, we have measured the relative differential cross section for each of the  $3p^5 4s$  ( $^3P_2$ ,  $^3P_1$ , and  $^3P_0$ ) levels at 0-4 eV above threshold, over scattering angles of  $90^\circ$ ,  $60^\circ$ ,  $30^\circ$ , and  $15^\circ$  (Wong, 1981).

Compared to the Kr experiments, the Ar experiments demand even higher sensitivity of the spectrometer. We have thus employed a newly developed apparatus, an electron-ion impact spectrometer, on its merits of having the necessary sensitivity and a large effective range of scattering angles.

This apparatus has been designed as a general purpose crossed-beam spectrometer for measurement of electron and ion impact cross sections relevant to the understanding of the physical mechanisms of electron collisional processes and to laser modelling. The scheme of the apparatus is illustrated in Fig. 12. It consists of a monochromator to generate a beam of monoenergetic

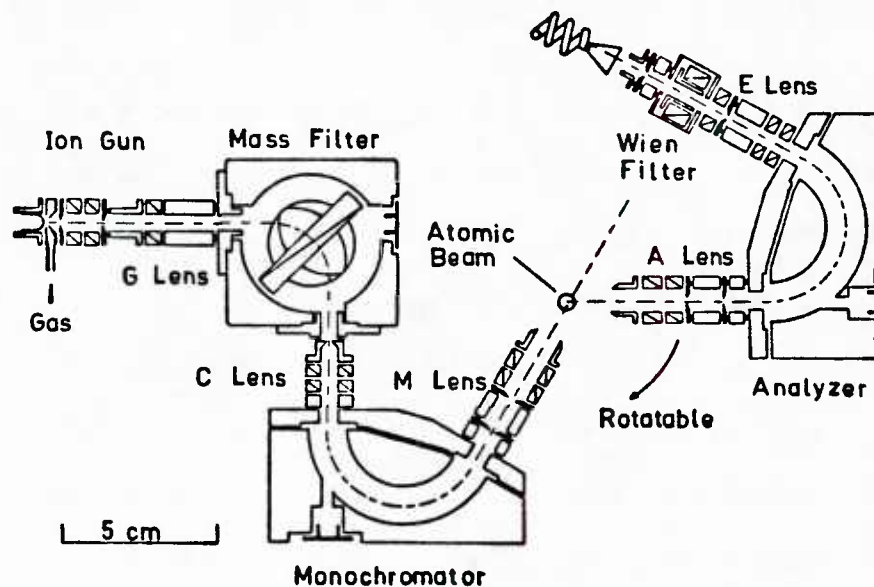


Fig. 12. Electron-ion impact spectrometer.  
(From Wong, 1981.)



electrons or mass-selected negative ions, a collision region in which this electron or negative-ion beam crosses an atomic beam, and a rotatable analyzer for measurement of the angular and energy distributions of the scattered electrons or ions. In the present experiments the resolution of the spectrometer is set to be 35 meV to facilitate separation of contributions from the 3 lowest excited levels in Ar. The maximum scattering intensity for these electronic processes is about 800 cps. The operation of this spectrometer has previously been described in the Final Technical Report for the NSF Grant PHY-78-00526 (Wong, 1983) and shall not be detailed here.

The experimental procedure we use to measure the relative electronic differential cross sections of Ar is essentially identical to that of Kr.

Fig. 13 shows the findings on these cross sections for the  $3P_2$ ,  $3P_1$ , and  $3P_0$  levels at  $90^\circ$ . The excitation to these 3 energy levels are all dominated by a broad resonant peak centered near 1.2 eV above threshold. Sharp resonant structures of varied shapes and magnitudes also appear in the vicinity of the broad peak. Of particular interest is that the gross shapes of the differential cross sections for the 3 levels mimic one another, with relative magnitudes consistent with their respective degeneracy factors, namely 5:3:1.

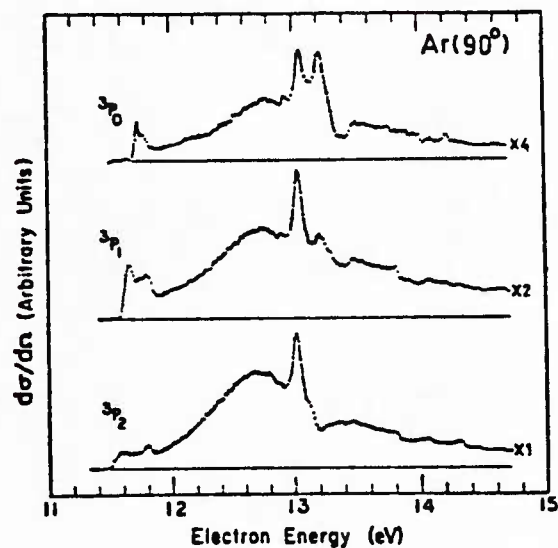


Fig. 13. Relative differential cross sections of the  $3P_0$ ,  $3P_1$ ,  $3P_2$  levels. (From Wong, 1981.)

Our results on the variation with angle of the differential cross sections for the lowest metastable level,  $^3P_2$ , and for the lowest UV emitting level,  $^3P_1$ , are presented in Figs. 14 and 15. Within the range of angles studied, the angular dependences of the overall magnitude of the metastable and the UV emitting levels are similar from 90 to 60° but differ in a major way at lower angles. In the metastable level, the overall magnitude is largest at 60°, but

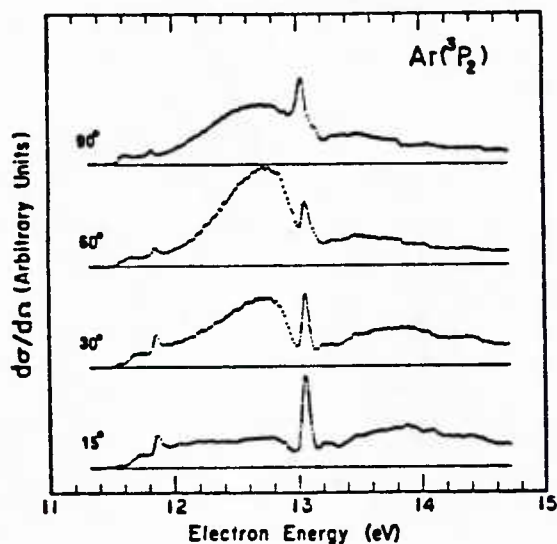


Fig. 14. Angular dependence of the  $^3P_2$  cross sections.  
(From Wong, 1981.)

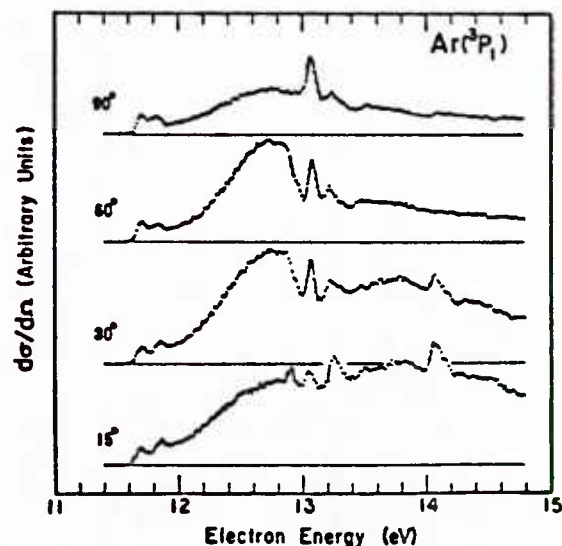


Fig. 15. Angular dependence of the  $^3P_1$  cross sections.

becomes smaller as the angle is lowered. On the other hand, in the UV emitting level, the overall magnitude rises steadily as the angle decreases below 60°, resulting the largest value at 15°.

### 3) Outlook on the Kr and Ar Experiments

Albiet the present near-threshold studies in Kr and Ar are in the initial phase of investigation, we have already observed a number of interesting phenomena, particularly the characteristic correlations among the differential



cross sections for the low lying energy levels in both atoms and the contrasting angular behavior between the lowest metastable and UV emitting levels in Ar. However, for laser modelling, further work on determination of the absolute magnitudes as well as on measurement of the angular dependences over a large range of observation angles ( $0-130^{\circ}$ ) are necessary.

In 1982, Yale University decided not to support further the experimental research in high-resolution electron scattering with atoms and molecules. We have then concluded our ongoing research for ONR at this stage.

#### IV. PUBLICATIONS UNDER ONR SPONSORSHIP

##### Articles:

Wong S F, Michejda J A and Stamatović A, "Resonant Electron Scattering from Vibrationally Excited N<sub>2</sub>," 10th Int. Conf. Electron. At. Collisions, abstracts p122 (1977)

Wong S F and Dubé L, "Rotational Excitation of N<sub>2</sub> by Electron Impact: 1-4 eV," Phys. Rev. A17, 570 (1978)

Tam W C and Wong S F, "Dissociative Attachment of Halogen Molecules by 0-8 eV Electrons," J. Chem. Phys. 68, 5626 (1978)

Wong S F, "Recent Trends in Beam Experiments on Dissociative Attachment," in Symposium on Electron-Molecule Collisions (Eds I Shimamura and M Matsuzawa, University of Tokyo, Tokyo) p111 (1979)

Allan M and Wong S F, "Dissociative Attachment from Vibrationally and Rotationally Excited HCl and HF," J. Chem. Phys. 74, 1687 (1981)

Phillips J M and Wong S F, "Electron Impact Excitation of He: Threshold Region," Phys. Rev. A23, 3324 (1981)

##### Invited Papers:

"Electron Scattering from Vibrationally Excited Molecules," Excited-State Workshop, 30th Gaseous Electronic Conference, Palo Alto, California (1977) (with J A Michejda and P D Burrow)

"Recent Trends in Electron-Beam Experiments," Current Status of Theory and Experiments in Electron-Molecule Scattering, Division of Electron and Atomic Physics, American Physical Society, Houston, Texas (1979)

"New Experiments on e-He and e-Ar Resonances," Symposium on Electron Scattering from Atoms and Atomic Ions, XII International Conference on the Physics of Electronic and Atomic Collision, Greenbelt, Maryland (1981)

## V. REFERENCES

1. Abouaf R and Teillet-Billy D, Chem. Phys. Lett. 73 106 (1980)
2. Allan M and Wong S F, J. Chem. Phys. 74 1687 (1981)
3. Bransden B H and McDowell M R C, Phys. Rep. 46 249 (1978)
4. Brau C A, in "Excimer Lasers" (Ed C K Rhode, Springer Verlag, Berlin) Chapter 4 (1979)
5. Chandra N and Temkin A, Phys. Rev. A14 507 (1976)
6. Chutjian A and Cartwright D C, Phys. Rev. A23 2178 (1981)
7. Dubé L and Herzenberg A, 9th Int. Conf. Electron. At. Collisions, abstracts (Eds J S Risley and R Geballe, University of Washington, Seattle) p264 (1975)
8. Kieffer L J, "A Compilation of Electron Collision Cross Section Data for Modelling Gas Discharge Lasers," JILA Report 13 (University of Colorado, Boulder, 1973)
9. Kurepa M V and Belić D S, Chem. Phys. Lett. 49 608 (1977)
10. LaBahn R W and Callaway J, Phys. Rev. A2 366 (1970)
11. Massey H S W, in "Negative Ions" (Cambridge University Press, Cambridge) Chapter 9 (1976)
12. McDaniel E W, Flannery M R, Ellis H W, Eisele F L, Pope W and Roberts T G, "Compilation of Data Relevant to Rare Gas-Rare Gas and Rare Gas-Monohalide Excimer Lasers," MIRADCOM Technical Report H-78-1, Volume II (1977)
13. Michejda J A, PhD Thesis, Yale University, New Haven (1977)
14. Phelps A V, Rev. Mod. Phys. 40, 399 (1968)
15. O'Malley T F, Burke P G and Berrington K A, J. Phys. B 12 953 (1979)
16. Phillips J M, PhD Thesis, Yale University, New Haven (1981)
17. Phillips J M and Wong S F, Phys. Rev. A23 3324 (1981)
18. Pichou F. Huetz A, Joyez G, Landau M and Mazeau J, J. Phys. B 9 933 (1976)
19. Read F H, J. Phys. B 5 255 (1972)
20. Schulz G J, in "Principles of Laser Plasmas," (Ed G Bekefi, Wiley Interscience, New York) Chapter 2 (1976)
21. Stamatović A and Schulz G J, J. Chem. Phys. 53 2663 (1970)

22. Swanson N, Cooper J W and Kuyatt C E, Phys. Rev. A8 1825 (1973)
23. Tam W C and Wong S F, J. Chem. Phys. 68 5626 (1978)
24. Trajmar S and Register D F, in "Electron Molecule Collisions," (Plenum Press, New York, 1980)
25. Trajmar S, Srivastava S K, Tanaka H and Nishimura H, Phys. Rev. A23 2167 (1981)
26. Wong S F, in "Symposium on Electron-Molecule Collisions," (Eds I Shimamura and M Matsuzawa, University of Tokyo, Tokyo) p111 (1979)
27. Wong S F, in "Symposium on Electron Scattering from Atoms and Atomic Ions," (Goddard Space Flight Center, Greenbelt) Invited Paper, (1981)
28. Wong S F, "Resonant Processes in Electron Scattering," Final Technical Report to NSF (Yale University, New Haven, 1983)
29. Wong S F and Dubé L, Phys. Rev. A17 570 (1978)
30. Wong S F, Michejda J A and Stamatović A, 10th Int. Conf. Electron. At. Collisions, abstracts (Commissariat a l'Energie Atomique, Paris) p122 (1977)
31. Wong S F and Schulz G J, Phys. Rev. Letters 32 1089 (1974)
32. Ziesel J P, Nenner I and Schulz G J, J. Chem. Phys. 63 1943 (1975)

U211911



C991

